Supplementary information for

Trajectory engineering of directrons in liquid crystals via photoalignment

Ke-Hui Wu[a], Chang-Qi Chen[a], Yuan Shen[b], Yu Cao[a], Sen-Sen Li[a,c], Ingo Dierking[b] and Lu-Jian Chen[a,c]**

[a] *Department of Electronic Engineering, School of Electronic Science and Engineering, Xiamen University, Xiamen 361005, China.*

[b] *Department of Physics and Astronomy, School of Natural Sciences, University of Manchester, Oxford Road, Manchester M13 9PL, UK.*

[c] *Fujian Key Laboratory of Ultrafast Laser Technology and Applications, Xiamen University, Xiamen, China.*

**Corresponding author(s). E-mail(s): sensenli@xmu.edu.cn; lujianchen@xmu.edu.cn*

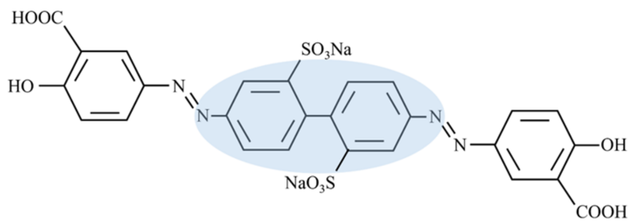

Supplementary Figure 1. Chemical structure of SD1.

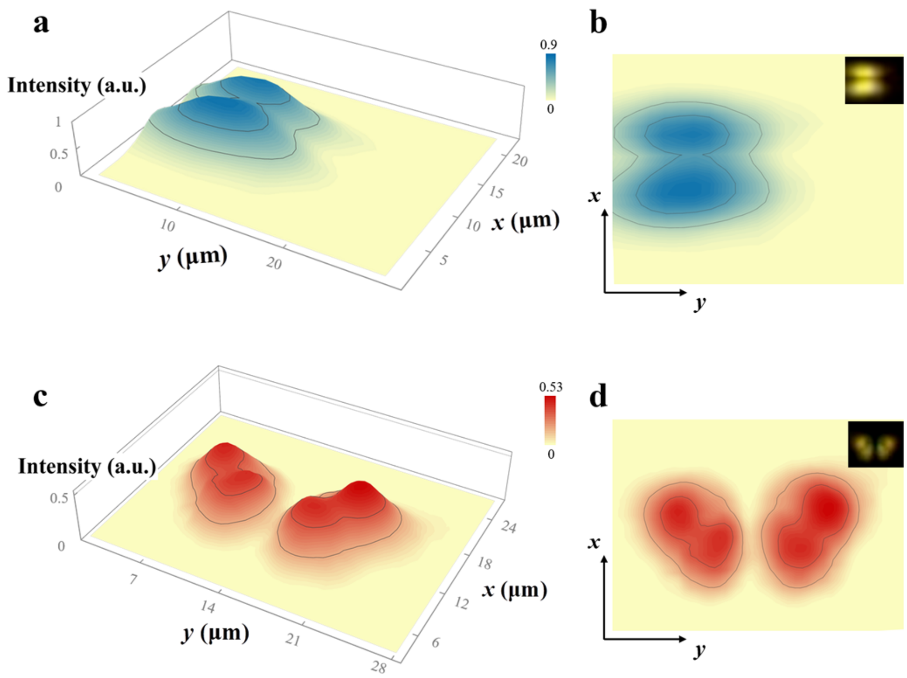

Supplementary Figure 2. The three-dimensional visualization of the (**a**) B_0^l and (**c**) B_{90}^l directrons, as well as in-plane images of (**b**) B_0^l and (**d**) B_{90}^l directrons. The insets show crossed polarizing optical microscopy (POM) of (**b**) B_0^l and (**d**) B_{90}^l directrons.

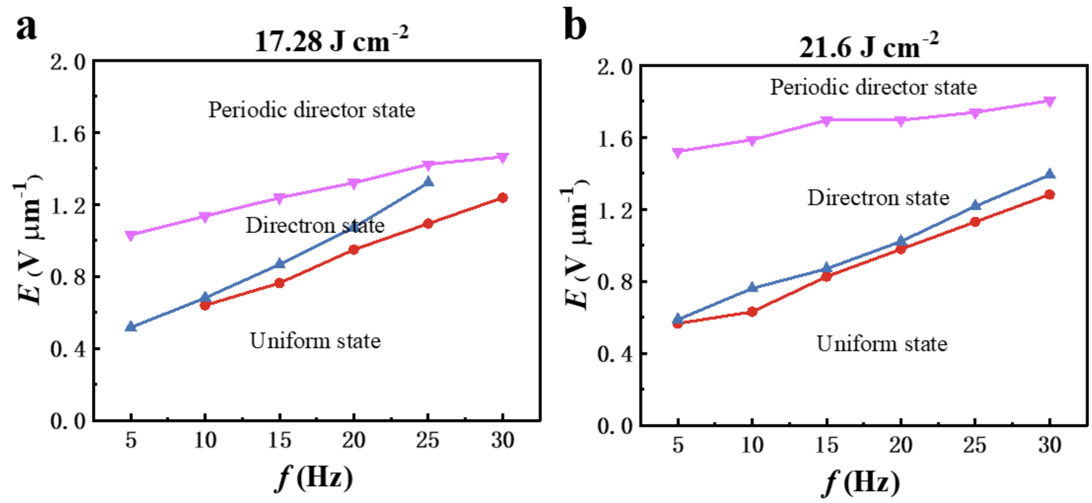

Supplementary Figure 3. *E*-*f* stability diagrams for exposure doses of (a) 17.28 J cm^{-2}, (b) 21.6 J cm^{-2} (Red, blue and purple lines represent the thresholds of B^{l}_{0} directron, B^{l}_{90} directron and periodic director state, respectively).

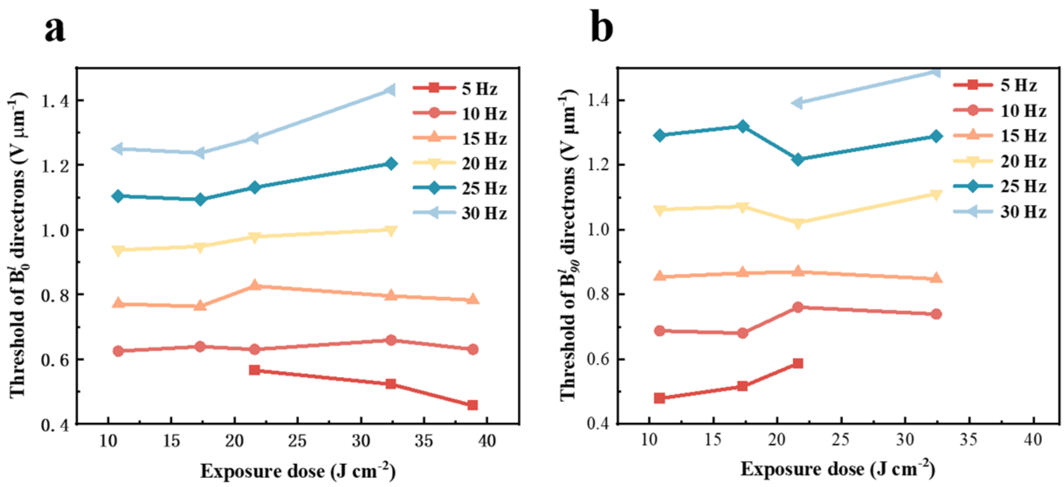

ss

Supplementary Figure 4. The generation threshold of (**a**) B^{l}_{0} directron and (**b**) B^{l}_{90} directron for varying exposure dose.

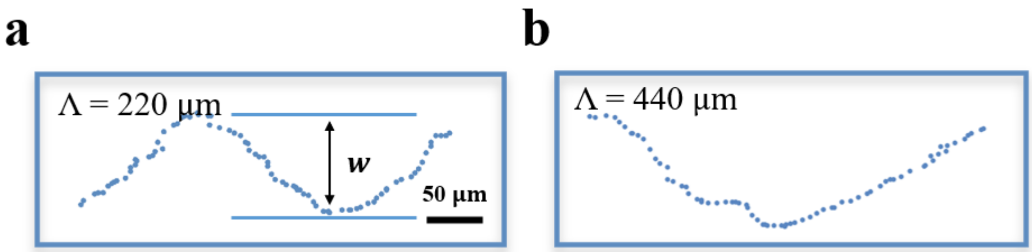

Supplementary Figure 5. The trajectories of B^{1}_{90} directrons for alignment periods of 220 μm (a), 440 μm (b). *w* and Λ are trajectory width and alignment period, respectively, the scale bar is 50 μm.

Transmittance of ITO coated glass substrates. During the exposure process, a linearly polarized light beam with a wavelength of λ = 405 nm passes through the top ITO coated glass substrate, the top SD1 alignment layer, the bottom SD1 alignment layer, and the bottom ITO coated glass substrate successively. The exposure light reaches the top SD1 alignment layer after passing through the top ITO coated glass substrate, then reaches the bottom one after continuing to pass through the top SD1 alignment layer. To evaluate the difference between the anchoring strengths of the top and bottom substrates, the transmittances of the ITO coated glass substrates, without and with the SD1 alignment layer, for the linearly polarized 405 nm light were measured, which are 87.1% and 80.0%, respectively. The single layer of SD1 absorbs approximately 7% of the linearly polarized 405 nm light. It is reasonable to infer that there is no significant difference between the anchoring strengths of the top and bottom substrates.

Sample preparation and testing. The experimental configuration of the cell, similar to that in the LC display, consists of the mixture of (-,-)-nematics CCN-47 and a small amount of TBAB which is sandwiched between two glass substrates. The combination of dielectric and conductive anisotropies is selected to preclude the two primary mechanisms of field-induced director reorientation, the dielectric torque and the standard Carr-Helfrich director instability[1]. The substrates are coated with indium tin oxide (ITO) layers, which serve as transparent electrodes for electric field application. The substrates with homeotropic alignment were achieved by being immersed in 10 wt% Dimethyloctadecyl[3-(trimethoxysilyl)propyl] (DMOAP) (Sigma-Aldrich) solution for 20 min[2], then rinsed with deionized water for 2 min and heated in the oven for 6 h at 100°C to evaporate the water. While the substrates for planar alignment were prepared by spin-coating the ITO-coated glass plates with a photoalignment layer of azo dye SD1. We used UV glue doped with 7 wt% 10 μm spacers[3] to assemble pairs of substrates to cells. The cell thicknesses vary from d = 8.8 μm to d = 10.5 μm, which was measured by the thin film interference method[4]. The empty cells for planar alignment were processed by photoalignment. Then, all empty cells were filled with the mixture sample. The anisotropies of dielectric permittivity and conductivity were measured by a dielectric spectrometer (Tonghui, TH2839) with planar and homeotropic alignment at an applied voltage of 0.1 V much lower than the threshold voltage for the electric Freedericksz transition, and at a frequency of 5 kHz[5,6]. The dielectric constants and conductivities of the LC mixture are $\varepsilon_P = 2.954$ and $\varepsilon_\perp = 8.565$,

$\sigma_P = 1.785 \times 10^{-9}\ \Omega^{-1}m^{-1}$ and $\sigma_{\perp} = 5.626 \times 10^{-9}\ \Omega^{-1}m^{-1}$, respectively. The subscripts // and $\perp$ indicate parallel and perpendicular to the director n_0.

Preparation of patterned cells. The LC cell substrate was photo-alignment using the polarization holography alignment technique, with two coherent waves of OLPs and OCPs to realize zigzag and fishhook-shaped trajectories, respectively. The quality of interference in the polarization holography photoalignment process is crucial to ensure the proper trajectory of directrons. In experiments, we used crossed POM to assess the quality of interference. The periodic dark stripes in POM images with half of the interference period indicate good interference quality.

Generation of directrons. The samples were heated to 55°C by a hot stage (Linkam, PE 94), and an AC field was applied across samples by a waveform generator (Rigol, DG1022) in combination with a power amplifier (FLC Electronics, A400DI). A sinusoidal or rectangular AC field is applied to the cell, $\boldsymbol{E} = (0,0,E)$ and f = 1-50 Hz to generate the directrons.

Optical characterization of directrons. Samples were observed in a polarizing optical microscope (Leica DM750P) equipped with a digital camera (Sony, E3ISPM20000KPA). The videos were recorded via Capture software at a frame rate of 10.8 fps.

***E-f* stability diagrams.** *E-f* stability diagrams were obtained by observing a region (900 μm × 450 μm) in the centre of the electrode edge by POM. The voltage amplitude was increased gradually (at a rate of 0.02 V μm^{-1} per 20 s) from an amplitude $\boldsymbol{E}$ far below the generation threshold of the directrons at constant frequency f. The threshold electric field was determined as amplitude E, at which first directrons could be observed by POM. The procedure was then repeated at different frequencies.

Trajectory measurement. The directron trajectories were analyzed by open-source software ImageJ and its plugin Manual mate and TrackMate, for manual or automated tracking, depending on the requirements of the experimental situation.

Supplementary Movie 1. Zig-zag trajectories of B^{1}_{90} directron with the alignment period Λ of 220 μm.

Supplementary Movie 2. Evolution of the periodic zigzag mode of B_{90}^{l} directron controlled by alignment periods. (**a**) 60 μm, (**b**) 110 μm, (**c**) 160 μm.

Supplementary Movie 3. The fishhook-shaped trajectory of B_{0}^{l} directron with the alignment period Λ of 160 μm.

Reference

1 Li, B.-X., Borshch, V., Xiao, R.-L., Paladugu, S., Turiv, T., Shiyanovskii, S. V. & Lavrentovich, O. D. Electrically driven three-dimensional solitary waves as director bullets in nematic liquid crystals. *Nat. Commun.* **9**, 1-10 (2018).

2 Shuzhen, Liao, Huazhi, Ding, Yan, Wu, Zhaoyang, Wu, Guoli & Shen. Label-free liquid crystal biosensor for L-histidine: A DNAzyme-based platform for small molecule assay. *Biosens. Bioelectron.* **79**, 650-655 (2016).

3 Ma, L.-L., Li, S.-S., Li, W.-S., Ji, W., Luo, B., Zheng, Z.-G., Cai, Z.-P., Chigrinov, V., Lu, Y.-Q., Hu, W. & Chen, L.-J. Rationally Designed Dynamic Superstructures Enabled by Photoaligning Cholesteric Liquid Crystals. *Adv. Opt. Mater* **3**, 1691-1696 (2015).

4 Xinyu, Zhu, Wing-Kit, Choi, Shin-Tson & Wu. A Simple Method for Measuring the Cell Gap of a Reflective Twisted Nematic LCD. *IEEE Trans Electron Devices* **11**, 1863-1867 (2002).

5 Dhara, S. & Madhusudana, N. V. Physical characterisation of 4′ -butyl-4-heptyl- bicyclohexyl-4-carbonitrile. *Phase. Transit.* **81**, 561-569 (2008).

6 Krekhov, A., Pesch, W. & Buka, A. Flexoelectricity and pattern formation in nematic liquid crystals. *Phys Rev E Stat Nonlin Soft Matter Phys* **83**, 051706 (2011).